

# Optically-pumped saturable absorber for fast switching between continuous-wave and passively mode-locked regimes of a Nd:YVO<sub>4</sub> laser

V.G. Savitski\*, D. Burns and S. Calvez

*Institute of Photonics, University of Strathclyde, 106 Rottenrow, Glasgow G4 0NW, UK*

\*Corresponding author: [vasili.savitski@strath.ac.uk](mailto:vasili.savitski@strath.ac.uk)

**Abstract:** We report on the fast (~50 μs) remote-controlled switching between continuous-wave (cw), cw mode-locked (ML) and Q-switched ML modes of operation of a Nd:YVO<sub>4</sub> laser using an optically-pumped saturable absorber (SA). Pulses as short as 40 ps with an average output power of 0.5 W are obtained in cw ML regime.

© 2009 Optical Society of America

**OCIS codes:** (140.3530) Lasers, neodymium; (140.4050) Mode-locked lasers; (140.3580) Lasers, solid-state.

---

## References and links

1. M. E. Fermann, A. Galvanauskas, and G. Sucha, "Ultrafast Lasers: Technology and applications," Marcel Dekker Inc, ISBN 0-8247-0841-5 (2003).
2. F. Dausinger, F. Lichtner, and H. Lubatschowski, "Femtosecond Technology for technical and medical applications," *Top. Appl. Phys.* **96**, Springer, ISBN 3-540-20114-9 (2004).
3. D. Stevenson, B. Agate, X. Tsampoula, P. Fischer, C. T. A. Brown, W. Sibbett, A. Riches, F. Gunn-Moore, and K. Dholakia, "Femtosecond optical transfection of cells: viability and efficiency," *Opt. Express* **14**, 7125-7133 (2006).
4. B. Agate, C. Brown, W. Sibbett, and K. Dholakia, "Femtosecond optical tweezers for in-situ control of two-photon fluorescence," *Opt. Express* **12**, 3011-3017 (2004).
5. J. Ando, G. Bautista, N. Smith, K. Fujita, and V. R. Daria, "Optical trapping and surgery of living yeast cells using a single laser," *Rev. Sci. Instrum.* **79**, 103705-103705-5 (2008).
6. W. Seitz, R. Ell, U. Morgner, T. R. Schibli, F. X. Kärtner, M. J. Lederer, and B. Braun, "All-optical active mode locking with a nonlinear semiconductor modulator," *Opt. Lett.* **27**, 2209-2211 (2002).
7. M. Guina and O. G. Okhotnikov, "Harmonic mode locking by synchronous optical pumping of a saturable absorber with the residual pump," *Opt. Lett.* **28**, 358-360 (2003).
8. S. Hais, M. Getbehead, and A. Pirich, "Q-switched / CW pulse trains produced by mode-locked fiber laser," *Proc. SPIE* **4042**, 17-23 (2000).
9. A. McWilliam, A. A. Lagatsky, C. T. A. Brown, W. Sibbett, A. E. Zhukov, V. M. Ustinov, A. P. Vasil'ev, and E. U. Rafailov, "Quantum-dot-based saturable absorber for femtosecond mode-locked operation of a solid-state laser," *Opt. Lett.* **31**, 1444-1446 (2006).
10. B. Stormont, E. U. Rafailov, I. G. Cormack, A. Mooradian, and W. Sibbett, "Extended-cavity surface-emitting diode laser as active mirror controlling modelocked Ti:sapphire laser," *Electron. Lett.* **40** (2004).
11. S. Giet, C. -L. Lee, S. Calvez, M. D. Dawson, N. Destouches, J. -C. Pommier, and O. Parriaux, "Stabilization of a semiconductor disk laser using an intra-cavity high reflectivity grating," *Opt. Express* **15**, 16520-16526 (2007).
12. N. Hempler, J. M. Hopkins, A. J. Kemp, N. Schulz, M. Rattunde, J. Wagner, M. D. Dawson, and D. Burns, "Pulsed pumping of semiconductor disk lasers," *Opt. Express* **15**, 3247-3256 (2007).
13. W. Koechner, *Solid-state laser engineering* (Springer USA 2006).
14. A. J. Kemp, G. J. Valentine, J. M. Hopkins, J. E. Hastie, S. A. Smith, S. Calvez, M. D. Dawson, and D. Burns, "Thermal management in vertical- external-cavity surface-emitting lasers: Finite-element analysis of a heatspreader approach," *IEEE J. Quantum Electron.* **41**, 148-155 (2005).
15. D. Burns, M. Hetterich, A. I. Ferguson, E. Bente, M. D. Dawson, J. I. Davies, and S. W. Bland, "High-average-power (>20-W) Nd:YVO<sub>4</sub> lasers mode locked by strain-compensated saturable Bragg reflectors," *J. Opt. Soc. Am. B* **17**, 919-926 (2000).
16. C. Hönninger, R. Paschotta, F. Morier-Genoud, M. Moser, and U. Keller, "Q-switching stability limits of continuous-wave passive mode locking," *J. Opt. Soc. Am. B* **16**, 46-56 (1999).

## 1. Introduction

In the last fifteen years, ultrafast mode-locked lasers have emerged as powerful scientific tools for laboratory-based applications such as: high-resolution metrology; material micro-machining; nonlinear spectroscopy and imaging of biological tissues, chemical species, semiconductor materials and devices [1-2]. In almost all of these uses, the source is operated continuously in a pulsed regime with fixed pulse characteristics. However, many applications, including photo-poration of trapped cells [3], optical tweezing [4] or chemical analysis, would benefit from a more versatile, user-friendly laser. Ideally, such a source would be able to be controllably switched between its continuous-wave (*cw* and *cw* mode-locked (ML)) regimes on short time scales, and also have its pulse parameters varied arbitrarily. For example, in photo-poration of cells, a *cw* beam is used for trapping and manipulation and the ultrashort pulse mode is used to puncture the cells [3]. Further, optical tweezing of particles could be supplemented with controllable two-photon luminescence by rapid switching to an ultrashort pulse probe [4], allowing a new imaging modality of the trapped cells. Recently, a dual-mode Ti:sapphire laser has been employed for manipulation (in the *cw* regime) and dissection (in the ultrashort pulse regime) of living yeast cells [5]. Therefore, it is clear that benefits can be derived from laser mode of operation switching in novel imaging and manipulation schemes.

Such operational regime changes have been demonstrated in actively ML lasers [6, 7], however, electronic modulators complicate the system and increase the cost and size - it is less clear how to implement this modality in passively modelocked lasers. Mechanical methods [5, 8, 9] have been exploited in passively ML lasers, but the resulting switching time is generally rather long (ms to s) and stringent laser alignment is required. In an attempt to overcome these drawbacks, Rafailov et al. [10] introduced a voltage-controlled resonant semiconductor saturable absorber mirror (SESAM) inside a Ti:sapphire laser and obtained switching between the *cw* and *cw* ML regimes. In the ML regime, the sign and magnitude of the applied bias controlled the pulse width (1.3 ns – 330 ps) and emission wavelength (940-960 nm), however, the mechanisms responsible for these dependencies were not explicitly examined.

In the present paper, we demonstrate the use of an optically-pumped saturable absorber (SA) inside a Nd:YVO<sub>4</sub> laser as a viable alternative method to remotely control the laser mode of operation. Switching with a fast (50μs) transient time between the *cw*, *cw* ML and Q-switched (QS) ML states is also obtained.

## 2. Experimental results

The laser cavity design shown in Fig. 1 was configured to enable stable high-power *cw* operation and to conveniently test different saturable absorber devices. The pump source was a 20-W fiber-coupled diode-laser array (DLA) operating at 808 nm. The gain medium was an 8 mm long Nd:YVO<sub>4</sub> crystal having 0.4% Nd concentration, and anti-reflection coated surfaces at ~1064 nm. The reflectivity of the output coupler was kept constant throughout the experiment at a value of 90%. The focusing mirror, M4, had a ROC of 75 mm and provided a mode diameter on the SA of 65 μm. An additional 808 nm External Diode Laser (EDL) delivering an incident power of up to 1.7 W onto the SA in a 150 μm-diameter spot was used to control the mode of operation of the laser. The larger spot size of the EDL was used as it simplified the alignment to the intracavity laser spot on the SA – closer matching would, of course, reduce the required EDL power.

The SA, originally designed as the active region of a semiconductor disk laser [11], consisted of a  $5\lambda$  GaAs-based cavity containing 10 strain-compensated In<sub>0.28</sub>Ga<sub>0.72</sub>As/GaAs<sub>0.9</sub>P<sub>0.1</sub> quantum-wells (QWs) (one per antinode) grown on top of a 35.5-pair AlAs/Al<sub>0.2</sub>Ga<sub>0.8</sub>As Distributed Bragg Reflector – the SA structure was capped by a  $3\lambda/2$  Al<sub>0.3</sub>Ga<sub>0.7</sub>As confinement window and a 10nm GaAs layer to prevent surface oxidation. At the chosen pump wavelength, carriers are generated throughout the GaAs cavity of the SA – a configuration typically referred to as barrier-pumping.

The laser was initially configured using an HR mirror instead of the SA. CW laser action with an incident pump threshold of 2.5 W, a slope efficiency of 17% and a pump-power limited, output power of 3.2 W was recorded.

Substituting the HR mirror with the SA, *cw* laser operation was achieved by cooling the SA mount to -10°C with a thermo-electric cooler. In order to prevent water condensation on the SA, dry nitrogen gas was flowed over the sample. In this configuration, the output power was recorded as 0.5 W for 11 W of pump power. Increasing the pump power above 11 W with no external pump power applied to the SA led to Q-switching instabilities and optical damage of the absorber.

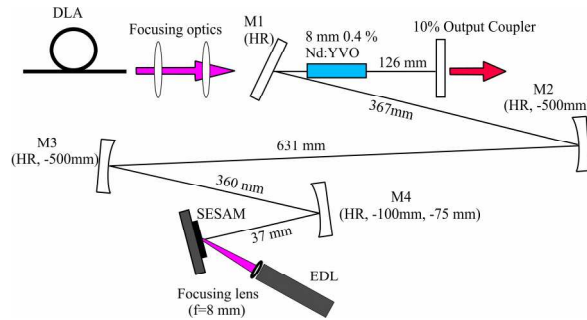


Fig. 1. Schematic of the experimental setup.

At a pump power of 6W, ML operation (at 93 MHz) of the laser was successfully obtained for 0.74 W EDL pumping of the SA (see Fig. 2) - increasing the EDL power to 0.89 W provoked QS-ML operation. The EDL power necessary to promote a given operational state was dependent on the laser pump power – this dependence was mapped and is presented as Fig. 3(a). As the laser pump power increases, the EDL power required to promote ML (and QS-ML) operation decreases, furthermore, the region of *cw* ML is enlarged. We also note that the SA suffered permanent damage at the highest laser pumping levels just above the onset of QS-ML (open symbol in Fig. 3(b)). Optimisation of the pumping powers (10 W DLA and 0.3 W EDL) led to a *cw* ML emission with a maximum output power of 0.5 W - the slope efficiency was 6.5%, the reduction over the original laser being reflective of the non-saturable losses introduced by the SA device. The output pulse duration, measured by intensity autocorrelation, was 40 ps, and the spectral width was 0.04 nm centred at 1064.4 nm – the duration-bandwidth product was therefore  $\sim 0.37$ , i.e. close to the Fourier-transform limit. No significant dependence of these pulse parameters with the EDL power was observed.

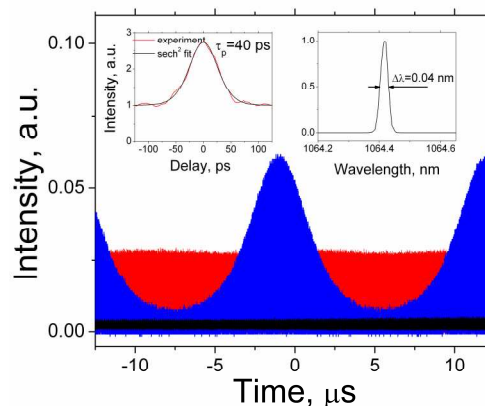


Fig. 2. Typical Nd:YVO<sub>4</sub> laser output traces under different external pump powers applied to the SA (0 W – black line, 0.74 W – red line, 0.89 W – blue line) and fixed pump power of the laser crystal (6 W). Inset: left – intensity autocorrelation trace of the *cw* ML pulse, right – corresponding optical spectrum.

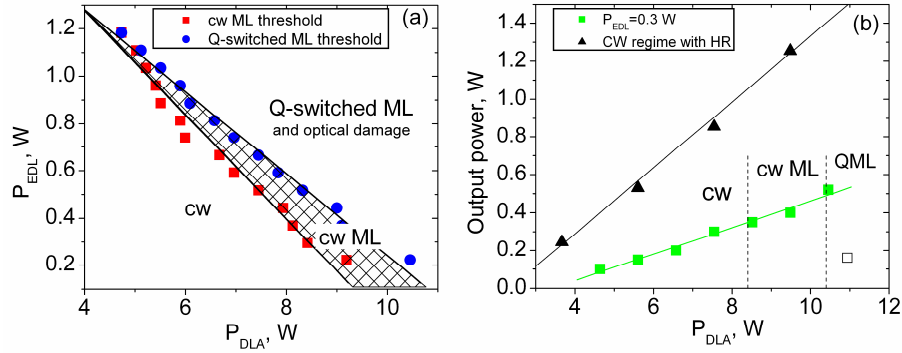


Fig. 3. (a) Map of laser oscillation state dependence on DLA and EDL power. The shaded region corresponds to the *cw* ML regime. (b) Nd:YVO<sub>4</sub> laser output power as a function of DLA power at constant EDL power = 0.3 W. Open symbol corresponds to optical damage of the SA. (The power transfer characteristic of the Nd:YVO<sub>4</sub> laser with the SA replaced by an HR mirror is shown for comparison.)

The typical behaviour of the Nd:YVO<sub>4</sub> laser when the SA was pulsed pumped to induce switching between *cw* and *cw* ML regimes is shown in Fig. 4. From this measurement a typical transition time of ~50-70 μs for switching between the different modes of operation of the laser was deduced. Here, the switching time is defined as the time between the turn-on of the EDL and the time at which the *cw* background is eliminated from the output signal. As this type of semiconductor device is characterised by a very fast heating rate (e.g. ~0.35K/ns for a GaSb-based device [12]), we believe the build-up time measured here is largely related to the number of round trips required to establish the stable *cw* ML state – generally, for solid state lasers, this is taken as >1500 round trips [13] i.e. ~ 15-20 μs in our case. Residual pulse energy variations in *cw* ML laser output after 70 μs were noted, possibly due to power variations in the EDL or temperature and gain adjustments in the Nd:YVO<sub>4</sub> crystal.

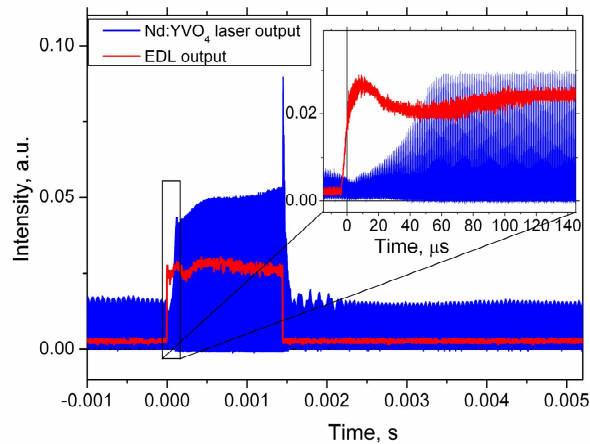


Fig. 4. Typical temporal response of rapid state-switching of the Nd:YVO<sub>4</sub> laser (blue). The applied EDL control pulse is also shown (red).

When the external pump is turned off, the cavity loss decreases rapidly. The laser then tends towards a new equilibrium state by way of relaxation-oscillation-induced spiking (observed just after external output terminates – see Fig. 4). It is apparent that the first “spike” contains picosecond pulses; however, subsequent features modulate the *cw* state as seen in the Fig. 4.

At a pump power of 8 W, with no external power applied, stable *cw*, *cw* ML and QS ML operation of the laser occurred when the SA mount temperature was set to -10, +1 and +12°C respectively. Thermo-electric-cooler induced switching was therefore possible; however, the switching transition time was on the order of 1 to 3s - i.e. over 5 orders of magnitude longer than the fast optically-induced state switching.

### 3. Discussion

In this section, we discuss the mechanisms involved in the control of the laser, the prospects for improving the laser performance and the design of a user-friendly versatile SA device. As the typical gain bandwidth of Nd:YVO<sub>4</sub> is ~1 nm, the discussion will assume that the laser wavelength is fixed at 1064.4 nm.

Optical pumping of the SA leads to (i) a reduction of the QW transition energy (due to heating) (ii) a faster recovery time due to increased non-radiative recombination at high temperatures and (iii) a broadening and a reduction in the strength of the QW excitonic absorption (due to band-filling and heating). Of these three effects, the first one is believed to play the most significant role in the configuration described here. This is indeed consistent with the observation that *cw* operation was only observed when the SA mount was cooled sufficiently to shift the QW absorption away from the laser wavelength. The initial absorption spectrum of the SA in this situation is shown in Fig. 5 with the blue solid line. As the pumping of the SA is increased, its internal temperature rises, and, accordingly, the saturation fluence (at 1064.4nm) decreases (as indicated in Fig. 5). This in turn results in the laser mode of operation moving successively from *cw* to *cw* ML. This is further verified by changing the temperature of the unpumped SA using only the TEC controlled mount – for DLA power of 8 W. The SA absorption spectrum under pumped (or unpumped, but TEC heated to +1°C) conditions, corresponding to *cw* ML regime of the laser, is presented in Fig. 5 as the green dashed line. Finally, as the EDL pumping (or TEC temperature) is increased further (TEC temperature of +12°C), the QS-ML regime is observed (relating to the red dotted line in Fig. 5). As this SA device is a resonant micro-cavity [11] the shift in absorption with temperature is modified and increases at a rate of 0.1 nm/°C.

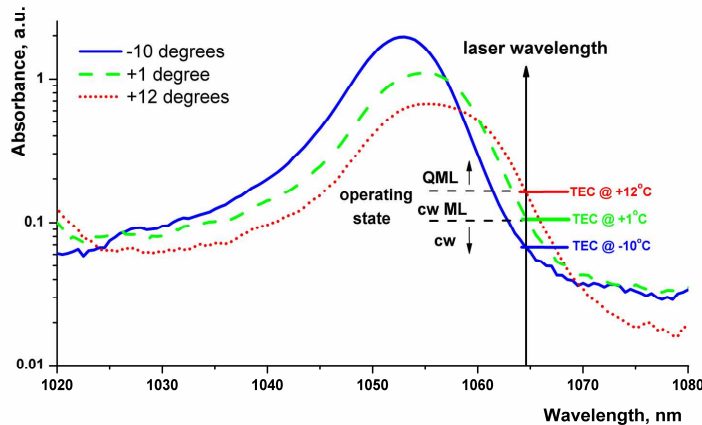


Fig. 5. Absorption spectra of the saturable absorber recorded at  $T = -10, 1, 12$  °C respectively. At the laser wavelength, the absorption varies significantly with device temperature. This temperature dependence of the absorption coefficient relates directly to an inverse dependence in the saturation fluence of the device [16] – this dependence can then be exploited to vary the oscillation mode of the laser. From experimental data (dotted lines), the three cases shown here relate to the *cw*, *cw* ML, and QML laser oscillation states respectively.

A finite element thermal analysis of the SA [14] has been performed in order to evaluate the average temperature changes induced by EDL pumping, and to compare these figures with

those experimentally obtained by heating the device with the TEC. A full description of finite element analysis (FEA) of these devices is given in [12]. In order to calculate the average temperature of the device, integration over the laser mode profile (with the waist of 32.5  $\mu\text{m}$ ) on the SA has been performed. Modelling was carried out with the following experimental parameters: waist radius of the EDL emission on the SA – 75  $\mu\text{m}$ ; EDL pump power required for the laser switching to *cw* ML regime – 0.38 W; EDL pump power required for laser switching to QML regime – 0.6 W. These figures related to a DLA pump power of 8 W, see fig. 3 (a). The results of the FEA modelling reveal a change in the average SA temperature of 10 K between 0.38 and 0.6 W EDL pumping. This relates directly to the experimentally measured TEC temperature change (of 11 K) to induce the same state change.

Our phenomenological model is consistent with the experimental observations made in [15]. In particular, as the temperature of the SA is increased, the intracavity power required to switch from QS-ML to *cw* ML increases. Therefore, for a constant intracavity power, the laser output is switched from *cw* ML to QS-ML as the saturable absorber is heated. This phenomenon was attributed to the wavelength shift of the SA absorption spectrum with heating and the consequent increase in  $F_{\text{sat}}\Delta R$ , (where  $F_{\text{sat}}$  is the saturation fluence and  $\Delta R$  is the modulation depth). Furthermore, such switching of oscillation regimes is expected according to the theoretical analysis described in [16]. The critical intracavity pulse energy required for *cw*-modelocking is proportional to the square root of  $F_{\text{sat}}\Delta R$  of the SA. Therefore, one would expect that, with all other conditions fixed, the laser will tend towards operation in QS ML regime as the absorption coefficient of the SA is increased, as observed here.

The reduction in the slope efficiency of the laser when the SA is introduced is attributed to the non-saturable absorption losses of the current device. From an analysis of the change in threshold power, it was deduced that the SA introduces an additional 2.4% of loss to the cavity. At present, it is not clear why this background loss is so high – comparison with similar devices having one or two InGaAs quantum wells [15] would suggest this loss should be considerably lower. We confirmed that this loss is not the sum of saturable and non-saturable losses of the SA, but only the passive non-saturable loss by tuning the absorption spectrum sufficiently to short wavelengths such that the saturable component is minimal. Further spectroscopic investigation and quantum well number optimisation is therefore necessary to fully understand the nature of these non-saturable losses, and so, optimise the power performance in this switchable state system. Room temperature operation will also be possible through compositional tuning of the quantum well absorption; however, the use of a TEC controlled mount is very convenient and flexible.

#### 4. Conclusion

In conclusion, we have demonstrated a technique featuring an intra-cavity, optically-pumped SA to provide a flexible approach to rapid operational-mode control in passively modelocked lasers. Laser oscillation in continuous-wave, *cw* mode-locked and Q-switched mode-locked regimes could be accessed by varying the pump power on the SA. Furthermore, fast switching between each oscillation state was demonstrated with a switching time of  $\sim 50 \mu\text{s}$  – i.e.  $>5$  orders of magnitude faster than obtained by changing the SA mount temperature. The basis of this control technique has been attributed to local heating within the SA and the subsequent shift in the quantum well absorption. Further optically-pumped SA development will focus on optimising the efficiency and extending the technique to femtosecond lasers.

#### Acknowledgments

This research was supported by the Engineering and Physical Sciences Research Council (EPSRC) programme “Ultrafast Modular Lasers”.